Lessons Learned

Article *in* Journal of the Astronautical Sciences · January 2013

DOI: 10.1007/BF03321491

CITATIONS
7

READS
191

1 author:

Landis Markley
retired
175 PUBLICATIONS **5,770** CITATIONS

SEE PROFILE

The Journal of the Astronautical Sciences, Vol. 57, Nos. 1 & 2, January–June 2009, pp. 000–000

Lessons Learned[1,2]

F. Landis Markley[3]

Abstract

This paper is organized around three themes that have interested me over my career: covariance analysis, constrained estimation, and angular momentum. Both analytical and numerical approaches to covariance analysis are discussed. The section on constraints begins with general considerations arising from the nature of the rotation group before moving to Wahba's Problem and quaternion Kalman filters. The discussion of angular momentum includes its use in attitude determination and control as well as in the detection and diagnosis of spacecraft anomalies. Relevant illustrative examples are included.

Introduction

The purpose of computing is insight, not numbers.
R. W. Hamming, *Numerical Methods for Scientists and Engineers* (1962)

The completion of the development phase of a NASA mission is often accompanied by a "Lessons Learned" document to capture the steps that went wrong and those that went right. My intent in this paper is to mark this stage of my career with an analogous document, but to exercise my authorial prerogative by focusing on what went right. This paper has some overlap with my Brouwer lecture [1], but is much less personal and is organized topically instead of chronologically. It is structured around three dominant themes of my career: The Utility of Covariance Analysis, the Complexity of Constraints, and the Importance of Angular Momentum. I have attempted to emphasize general concepts rather than computational details and to illustrate each topic with relevant examples. The discussion is unavoidably technical in places, however.

The discussion of covariance analysis includes both analytical and numerical approaches [2–10]. The analytical part recounts Farrenkopf's expression for the steady-state attitude accuracy of a single-axis attitude estimator [3] and an extension of his result [7]. The numerical discussion relates the development of the Attitude Determination Error Analysis System (ADEAS) [8] and the role of ADEAS

[1]Presented at the F. Landis Markley Astronautics Symposium, Cambridge, Maryland, June 29–July 2, 2008.
[2]This paper is dedicated to Eugene J. Lefferts.
[3]Guidance, Navigation and Control Systems Engineering Branch, Code 591, NASA Goddard Space Flight Center, Greenbelt, MD 20771. E-mail: landis.markley@nasa.gov.

in leading by a circuitous path to a backup control mode for the Tropical Rainfall Measuring Mission (TRMM) [11, 12].

The section on constraints [4, 5, 13–40] begins with general considerations arising from the nature of the rotation matrix, and continues with discussions of Wahba's formulation of the attitude estimation problem [18] and of quaternion Kalman filters [4, 5, 28, 34–38]. This is the longest and most technical section of the paper and includes the only new material, which is relegated to an Appendix.

The last section of the paper covers the use of angular momentum for attitude determination of spinning spacecraft [41–45] and for attitude control [46–53]. The control applications discussed are the remarkably similar mission mode of the Solar, Anomalous, and Magnetospheric Particle Explorer (SAMPEX) [47–50] and gyroless safe pointing mode of the Hubble Space Telescope (HST) [51]. The paper closes with a discussion of the use of conservation of angular momentum to detect anomalous gyro behavior on HST [52] and to diagnose an anomaly on the Wilkinson Microwave Anisotropy Probe (WMAP) [53].

The Utility of Covariance Analysis

I learned to appreciate the value of covariance analysis from Gene Lefferts, my most important mentor in the aerospace field. In Kalman filtering, the covariance matrices $P_i(+)$ after the ith measurement, $P_i(-)$ before this measurement, and $P_{i-1}(+)$ after the previous measurement satisfy the well-known equations [2]

$$P_i(-) = \Phi(t_i, t_{i-1})P_{i-1}(+)\Phi^{\mathrm{T}}(t_i, t_{i-1}) + \int_{t_{i-1}}^{t_i} \Phi(t_i, t)Q(t)\Phi^{\mathrm{T}}(t_i, t)\mathrm{d}t \tag{1a}$$

$$K_i = P_i(-)H_i^{\mathrm{T}}[H_iP_i(-)H_i^{\mathrm{T}} + R_i]^{-1} \tag{1b}$$

$$P_i(+) = (I - K_iH_i)P_i(-) \tag{1c}$$

where Φ is the state transition matrix, Q is the power spectral density of the process noise, K_i is the Kalman gain, H_i is the measurement sensitivity matrix, and R_i is the measurement noise covariance. These equations have to be solved numerically in general. The covariance can approach steady state values $P_i(+) \Rightarrow P(+)$ and $P_i(-) \Rightarrow P(-)$ if the measurements are evenly spaced in time and have constant H and R, the process noise power spectral density is constant, and $\Phi(t, t')$ depends only on $t - t'$. Steady state solutions can be found numerically, or sometimes algebraically, by solving the coupled equations (1) for $P(+)$ and $P(-)$ under the stated assumptions. Solving these equations algebraically is an intractable problem for all but the simplest scenarios, but they become more manageable in the limit that the time interval Δt between the measurements is much less than the time constants of the filter. This is the limit that the update interval goes to zero while $R\Delta t$ approaches a constant. In this limit $\Phi(\Delta t, 0) \approx I + F\Delta t$ and the update from any one measurement is negligible, so $P(+)$ and $P(-)$ become equal. The steady-state covariance matrix satisfies the equation

$$0 = FP + PF^{\mathrm{T}} + Q - PH^{\mathrm{T}}(R\Delta t)^{-1}HP \tag{2}$$

This is the algebraic Riccati equation for the continuous-time Kalman filter, and it is much more amenable to analytic solution than the coupled equations (1). I have obtained very useful insights by finding the steady-state covariance of some simple cases, such as yaw gyrocompassing, but these cases are often too unphysical to be of practical use.

Farrenkopf's Equations

In 1978, Robert L. Farrenkopf found an algebraic solution for the steady-state covariance with a finite update interval in a very interesting case: single-axis attitude determination using a gyro and an angle sensor such as a star tracker [3]. The state vector contained the angle θ and the gyro drift bias b. The gyro was used in model replacement mode, meaning that gyro data replace Euler's equations in the dynamic propagation step instead of being treated as measurements. This model has been widely employed in spacecraft attitude estimation [4, 5]. The coupled steady-state covariance equations in Farrenkopf's model led to a quartic equation, but he found a factorization of the quartic into two quadratic equations, leading to an incredibly useful estimate of the accuracy of attitude estimation systems.

Farrenkopf's model included three error sources: gyro angle random walk σ_v, gyro rate random walk σ_u, and angle sensor measurement noise σ_n. Spacecraft generally use rate-integrating gyros, which have noise on the gyro output known as angle white noise that was not included in Farrenkopf's model [6]. This noise source is not important for many gyros, including those for which Farrenkopf's equations have usually been applied, but it can be significant for some newer gyros such as ring laser gyros. Kong Ha at Goddard Space Flight Center had found a way to incorporate angle white noise into gyro processing, but didn't look for a steady-state solution. In 2000, I discovered that including angle white noise led to a quartic equation that could be solved exactly like Farrenkopf's. I showed my original derivation of these results to Reid Reynolds, and together we found a better derivation for publication [7].

With σ_e denoting the standard deviation of the angle white noise, the components of the steady-state covariance matrix are

$$P_{\theta\theta}(\overline{+}) = \kappa^{\pm 1}(\kappa - \kappa^{-1})\sigma_n^2 \tag{3a}$$

$$P_{\theta b}(\overline{+}) = -\kappa^{\pm 1}\sigma_n\sigma_u(\Delta t)^{1/2} \tag{3b}$$

$$P_{bb}(\overline{+}) = \sigma_u\left[\sigma_v^2 + 2\tilde{\sigma}\sigma_u(\Delta t)^{1/2} + \frac{1}{3}\sigma_u^2(\Delta t)^2\right]^{1/2} \pm \frac{1}{2}\sigma_u^2\Delta t \tag{3c}$$

where

$$\kappa \equiv \sigma_n^{-1}\left\{\tilde{\sigma} + \frac{1}{4}\sigma_u(\Delta t)^{3/2} + \frac{1}{2}\left[\sigma_v^2\Delta t + 2\tilde{\sigma}\sigma_u(\Delta t)^{3/2} + \frac{1}{3}\sigma_u^2(\Delta t)^3\right]^{1/2}\right\} \tag{4a}$$

$$\tilde{\sigma} \equiv \left[\sigma_n^2 + \sigma_e^2 + \frac{1}{4}\sigma_v^2\Delta t + \frac{1}{48}\sigma_u^2(\Delta t)^3\right]^{1/2} \tag{4b}$$

Except for notation, these results are identical to Farrenkopf's if $\sigma_e = 0$.

As an example, consider a ring-laser gyro with very low drift but with significant angle white noise, for which $\sigma_v = 0.025\ \text{deg}/\sqrt{\text{hour}}$ and $\sigma_u = 3.7 \times 10^{-3}\text{deg/hour}^{3/2}$, and assume star tracker measurement noise with $\sigma_n = 15\ \mu\text{rad}$. Figure 1 shows the steady-state pre-update and post-update angle standard deviations, the square roots of $P_{\theta\theta}(\overline{+})$, for star tracker update times Δt between 0.01 sec and 100 sec. The solid curves are for $\sigma_e = 15\ \mu\text{rad}$, which is appropriate for this gyro, and the dashed curves are for $\sigma_e = 0$. For each pair of curves, the upper curve is the pre-measurement-update value, and the lower curve is the post-measurement-update value.

Figure 1 clearly shows that increasing the frequency of star tracker updates has less effect on the angle estimation accuracy when gyro output white noise is present.

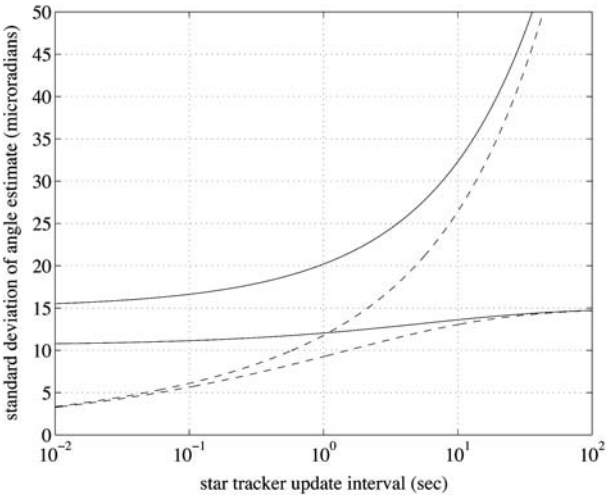

FIG. 1. Steady-state angle standard deviation.

The dashed lines show $P_{\theta\theta}(+)$ and $P_{\theta\theta}(-)$ approaching a common asymptote as the update interval goes to zero, but the solid curves do not exhibit this property. The reason for this is that the gyro process noise over the interval between measurements has contributions proportional to $(\Delta t)^{1/2}$ and $(\Delta t)^{3/2}$, but angle white noise gives a finite contribution as Δt goes to zero. This is a drawback of using gyros in the model replacement mode, because the actual spacecraft cannot rotate through a finite angle in zero time.

Attitude Determination Error Analysis System (ADEAS)

In 1987 I headed a team that developed the Attitude Determination Error Analysis System (ADEAS), a numerical attitude error covariance analysis program. ADEAS is still widely used at Goddard to predict the attitude estimation accuracy attainable with different sensor complements, different observation schedules, and different estimation methods, including mistuned estimators. My colleague in this effort was Ed Seidewitz, a brilliant recent MIT graduate. Ed and I worked through the covariance analysis equations for both batch estimators and Kalman filters with solve-for and consider parameters. Mark Nicholson did most of the programming, and also uncovered errors in the equations Ed and I gave him to code. I believe that much has been lost in the increasing separation of the functions of computer scientist and control engineer. The results of Ed's, Mark's, and my seamless collaboration were documented in a conference paper [8] but never published in an archival journal until now [9].

One of the innovations of ADEAS was its ability to assess the influence of process noise in a batch estimator. Figure 2 is a plot produced in Julie Thienel's (then Julie Deutschmann) analysis of the attitude accuracy of the Compton Gamma Ray Observatory [8]. This problem, which is not dominated by dynamics or observation geometry, has errors that are smallest near the center of the batch and larger at the ends. Process noise contributes to this characteristic shape often seen in batch estimators. The right-left asymmetry of the plot is due to assumed *a priori* attitude knowledge of 27 arc seconds at time zero. Figure 2 is also a nice illustration of the 1989 state-of-the-art in computer graphics.

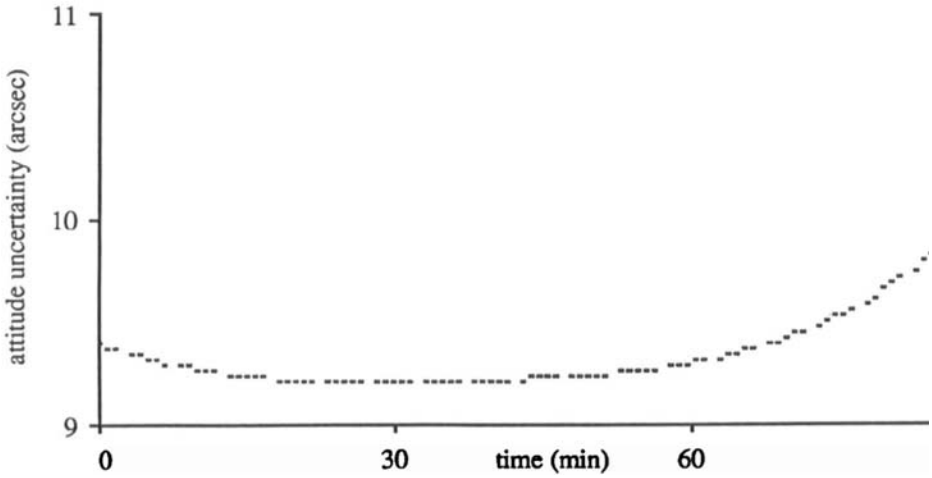

FIG. 2. Batch Estimation Accuracy Estimate for the Compton Gamma Ray Observatory.

Tropical Rainfall Measuring Mission (TRMM)

In 1991, Goddard embarked on the simultaneous development of two spacecraft in-house: the Tropical Rainfall Measuring Mission (TRMM) and the X-Ray Timing Explorer (XTE), later renamed RXTE in honor of Bruno Rossi. The two spacecraft used a common procurement for reaction wheels and gyros, but their attitude control systems were quite different. XTE chose a stellar-inertial attitude reference to satisfy its arcsecond pointing requirements [10], while TRMM chose an Earth-referenced system to satisfy its less stringent 0.3° (3σ) attitude knowledge requirement. TRMM employed a static Earth horizon sensor similar to that used on the NOAA and Defense Meteorological Satellite Program (DMSP) low-Earth-orbiting spacecraft. In early 1994, after development of the TRMM ACS was well underway, we became aware of a progressive loss of optical transmission through some of the windows of the DMSP horizon sensors. We worried that TRMM, with its lower 350 km altitude orbit, might experience a more severe problem, and possibly even complete loss of the attitude reference. To protect against this possibility, we considered adding a star tracker to TRMM, which would have incurred severe monetary and schedule penalties.

I knew that Joe Hashmall had found some very encouraging batch attitude determination results using flight gyro and magnetometer data from the Upper Atmosphere Research Satellite (UARS). Joe told me much later that he had first seen these promising results in an ADEAS covariance analysis, and believing them to be too good to be true, had turned to batch estimation in an unsuccessful effort to show that ADEAS contained an error. I asked Eleanor Ketchum, who was sponsoring Joe's work, whether his method could be adapted to a Kalman filter for attitude estimation onboard TRMM. They and Joe Sedlak responded enthusiastically, and within a month had developed a Kalman filter that gave 0.3° attitude accuracy using UARS data [11]. The Kalman filter requires a dynamic memory of approximately one orbit period to reduce the effects of magnetic field modeling errors. This memory is provided on TRMM by the precise gyros procured as part of a common buy with XTE, which were much more capable than had been required by the Earth-sensor-based

TRMM ACS. The TRMM Kalman filter was not used operationally until TRMM's orbit altitude was raised from 350 km to 402 km in 2001 to conserve propellant needed to compensate for atmospheric drag. The static Earth sensor that had performed according to specification at the lower altitude ceased providing valid data above 380 km, as had been expected. The Kalman filter was enabled and is now providing attitude accuracies of approximately 0.2°, about the same as the horizon sensor had provided [12].

The Complexity of Constraints

Constraints in Attitude Estimation

The fundamental constraint of attitude estimation is that the attitude matrix A is a member of the rotation group, or special orthogonal group SO(3). This is just the group-theoretical way of saying that A must be an orthogonal matrix with determinant $+1$. The orthogonality constraint

$$A^{\mathrm{T}}A = I_{3\times 3} \tag{5}$$

is nonlinear, which leads to the complications that make attitude estimation difficult but also make it interesting. In fact, the orthogonality constraint is very useful because it reduces the number of degrees of freedom to be estimated [13]. The kinematic equation for the attitude matrix is [14, 15]

$$\mathrm{d}A/\mathrm{d}t = -[\boldsymbol{\omega}\times]A \tag{6}$$

where

$$[\boldsymbol{\omega}\times] \equiv \begin{bmatrix} 0 & -\omega_3 & \omega_2 \\ \omega_3 & 0 & -\omega_1 \\ -\omega_2 & \omega_1 & 0 \end{bmatrix} \tag{7}$$

is the cross-product matrix. This kinematic equation preserves the orthogonality of A exactly with exact arithmetic.

Equation (5) is equivalent to six independent scalar constraints, not nine, because the matrix $A^{\mathrm{T}}A$ is symmetric. This means that the attitude matrix has three degrees of freedom. Many three-dimensional representations of rotations exist [15, 16], but it is well known that all three-parameter representations of SO(3) are singular or discontinuous for certain attitudes [17]. This has led to widespread use of the quaternion, the nonsingular parameterization with the lowest dimensionality [15, 16]. The quaternion is written in terms of a three-vector part $\mathbf{q}$ and a scalar part q_4 as

$$q = \begin{bmatrix} \mathbf{q} \\ q_4 \end{bmatrix} \tag{8}$$

and the attitude matrix is parameterized by

$$A(q) = (q_4^2 - \|\mathbf{q}\|^2)I_{3\times 3} + 2\mathbf{q}\mathbf{q}^{\mathrm{T}} - 2q_4[\mathbf{q}\times] \tag{9}$$

where $\|\cdot\|$ denotes the Euclidan vector norm. Straightforward algebra shows that equation (9) gives

$$A^{\mathrm{T}}(q)A(q) = \|q\|^4 I_{3\times 3} \tag{10}$$

where

$$\|q\|^2 = q_4^2 + \|\mathbf{q}\|^2 \tag{11}$$

Thus equation (9) represents an orthogonal matrix if and only if the quaternion satisfies the normalization condition

$$||q||^2 = 1 \tag{12}$$

which is also a nonlinear constraint. It is clear from equation (9) that q and $-q$ represent the same attitude. This nonuniqueness of the quaternion representation is a minor annoyance that cannot be removed without introducing discontinuities like those that plague three-dimensional attitude representations. The kinematic equation for the quaternion is [14, 15]

$$\mathrm{d}q/\mathrm{d}t = \frac{1}{2}\begin{bmatrix} \boldsymbol{\omega} \\ 0 \end{bmatrix} \otimes q \tag{13}$$

where we use the quaternion product that gives $A(q \otimes q') = A(q)A(q')$ [5, 15]. Equation (13) preserves quaternion normalization with exact arithmetic.

Before attacking the constrained estimation problem incorporating dynamics, we will first consider the static problem of finding the best estimate using vector measurements taken at a single point in time.

Wahba's Problem

In 1965, Grace Wahba posed the static attitude estimation problem as the problem of finding the proper orthogonal matrix that minimizes the loss function [18]

$$L(A) \equiv \frac{1}{2}\Sigma_i a_i ||\mathbf{b}_i - A\mathbf{r}_i||^2 = \frac{1}{2}\Sigma_i a_i (||\mathbf{b}_i||^2 + ||A\mathbf{r}_i||^2) - \Sigma_i a_i \mathbf{b}_i^{\mathrm{T}} A \mathbf{r}_i \tag{14}$$

where the sum is over the observations, $\mathbf{r}_i$ is a vector to an observed object in reference coordinates, $\mathbf{b}_i$ is the corresponding vector in the spacecraft body coordinates, and a_i is a non-negative weight assigned to the observation. The first term on the right side of equation (14) is independent of the attitude as a result of the orthogonality constraint, and the second term can be rewritten in terms of the matrix trace as

$$\Sigma_i a_i \mathbf{b}_i^{\mathrm{T}} A \mathbf{r}_i = \mathrm{trace}\,(AB^{\mathrm{T}}) \tag{15}$$

where B is the "attitude profile matrix"

$$B \equiv \Sigma_i a_i \mathbf{b}_i \mathbf{r}_i^{\mathrm{T}} \tag{16}$$

Thus Wahba's Problem is the problem of maximizing trace (AB^{T}). Using the Frobenius norm (also known as the Euclidean, Schur, or Hilbert-Schmidt norm) [19, 20]

$$||M||_{\mathrm{F}}^2 \equiv \Sigma_{i,j} M_{ij}^2 = \mathrm{trace}\,(MM^{\mathrm{T}}) \tag{17}$$

we see that

$$||A - B||_{\mathrm{F}}^2 = ||A||_{\mathrm{F}}^2 + ||B||_{\mathrm{F}}^2 - 2\mathrm{trace}\,(AB^T) = 3 + ||B||_{\mathrm{F}}^2 - 2\mathrm{trace}\,(AB^T) \tag{18}$$

This means that Wahba's Problem is equivalent to finding the orthogonal matrix A that is closest to B in the Frobenius norm. Wahba's Problem is a special case of the orthogonal Procrustes problem [19, 20]. We see that the orthogonality constraint on the attitude matrix is crucial in both equations (14) and (18).

In 1977, Paul Davenport found the first really useful solution of Wahba's Problem by substituting the quaternion representation of the attitude matrix into equation (15), giving [21]

$$\text{trace}[A(q)B^{\mathrm{T}}] = q^{\mathrm{T}}Kq \tag{19}$$

with

$$K \equiv \begin{bmatrix} B + B^{\mathrm{T}} - I_{3\times 3}\,\text{trace}\,B & \Sigma_i a_i \mathbf{b}_i \times \mathbf{r}_i \\ (\Sigma_i a_i \mathbf{b}_i \times \mathbf{r}_i)^{\mathrm{T}} & \text{trace}\,B \end{bmatrix} \tag{20}$$

Thus Wahba's problem is also equivalent to the maximization of $q^{\mathrm{T}}Kq$, which doesn't make any sense without the quaternion normalization constraint. Appending this constraint to equation (19) using a Lagrange multiplier is one way to derive Davenport's result that the optimal quaternion is the eigenvector of K with the maximum eigenvalue, i.e.

$$Kq_{\text{opt}} = \lambda_{\max} q_{\text{opt}} \tag{21}$$

Davenport's q method appeals to physicists who love to work with eigenvectors and eigenvalues.

Although very robust, Davenport's q method was very slow with the computers available at the time, leading Malcolm Shuster to develop his QUEST algorithm [22], which has been used in star trackers that determine their attitude autonomously. Many other algorithms have been developed since QUEST, including the SVD method [23], FOAM [24], and Daniele Mortari's ESOQ [25] and ESOQ2 [26] algorithms. As 1990 approached, Malcolm Shuster proposed that we write a survey paper entitled "25 Years of Wahba's Problem," but we never found the time to do it. In 1995 I gave a talk called, not surprisingly, "30 Years of Wahba's Problem." Daniele Mortari invited me to repeat this talk in Rome, which led to our paper surveying the different methods and comparing their speed and accuracy [27].

General Statistical Considerations

Before discussing Kalman filtering, let us explore some general statistical concepts. Consider a probability distribution of vectors defined on N-dimensional Euclidean space $\mathbb{R}^N$. We denote the average over the distribution, or the expectation, by an overbar,

$$\bar{\mathbf{x}} \equiv E[\mathbf{x}] \tag{22}$$

This is generally the best estimate of $\mathbf{x}$ in the absence of constraints. Suppose, though, that all the vectors in the probability distribution satisfy some nonlinear constraint such as the norm constraint on the quaternion, which we indicate as $\mathbf{x} \in S$, where S is the set in which the vectors are constrained to lie. The expectation will not satisfy the constraint in general, i.e. $\bar{\mathbf{x}} \notin S$. This has led to the erroneous belief that pdfs on non-Euclidean manifolds necessarily yield unphysical estimates [28]. In contrast to this, Oshman and Carmi [29] have emphasized that either the minimum mean-square error (MMSE) estimate or the maximum likelihood estimate (MLE) can provide a perfectly valid attitude estimate satisfying a nonlinear constraint.

The MMSE estimate, denoted by a caret, is defined as

$$\hat{\mathbf{x}} \equiv \underset{\mathbf{x}' \in S}{\arg\min}\, E\left[\|\mathbf{x}' - \mathbf{x}\|^2\right] \tag{23}$$

where $\mathbf{x}'$ is regarded as a constant vector while computing the expectation. Note that the definition of $\hat{\mathbf{x}}$ requires it to satisfy the constraint. Substituting $\mathbf{x}' - \mathbf{x} = (\mathbf{x}' - \bar{\mathbf{x}}) - (\mathbf{x} - \bar{\mathbf{x}})$ into equation (23), we see that

$$\hat{\mathbf{x}} \equiv \underset{\mathbf{x}' \in S}{\arg\min} \{E[\|\mathbf{x}' - \bar{\mathbf{x}}\|^2] + E[\|\mathbf{x} - \bar{\mathbf{x}}\|^2] - 2E[(\mathbf{x}' - \bar{\mathbf{x}}) \cdot (\mathbf{x} - \bar{\mathbf{x}})]\}$$

$$= \underset{\mathbf{x}' \in S}{\arg\min} \|\mathbf{x}' - \bar{\mathbf{x}}\|^2 \tag{24}$$

The second equality follows because $\mathbf{x}' - \bar{\mathbf{x}}$ does not depend on $\mathbf{x}$, $E[\|\mathbf{x} - \bar{\mathbf{x}}\|^2]$ does not depend on $\mathbf{x}'$, and $E[\mathbf{x} - \bar{\mathbf{x}}] = 0$ by the definition of $\bar{\mathbf{x}}$. Thus $\hat{\mathbf{x}}$ is the closest vector in S to $\bar{\mathbf{x}}$. We note that if there is no constraint, i.e. if $S \equiv R^N$, then the MMSE estimate is obviously identical to the expectation.

The MLE is simply defined as the point in the distribution where the probability reaches a maximum, assuming that this point is unique. Shuster has shown that Wahba's Problem can be understood as a maximum likelihood estimation problem [30].

In the special case that the constraint is a norm constraint $\|\mathbf{x}\| = 1$, a little thought shows that $\|\bar{\mathbf{x}}\| < 1$ in general because all the vectors in the probability distribution are assumed to obey the constraint. In this case equation (24) gives the MMSE estimate as $\hat{\mathbf{x}} = \bar{\mathbf{x}}/\|\bar{\mathbf{x}}\|$.

As a concrete example of these concepts, consider the distribution of vectors in a plane illustrated in Fig. 3. All the vectors are required to lie on the unit circle, and the density of points along the arc, illustrated by the width of the thick line, is

$$p(x, y) = (2/\pi)(1 + y)(1 - y^2) \qquad \text{for x} \geq 0 \tag{25a}$$

$$p(x, y) = 0 \qquad \text{for x} < 0 \tag{25b}$$

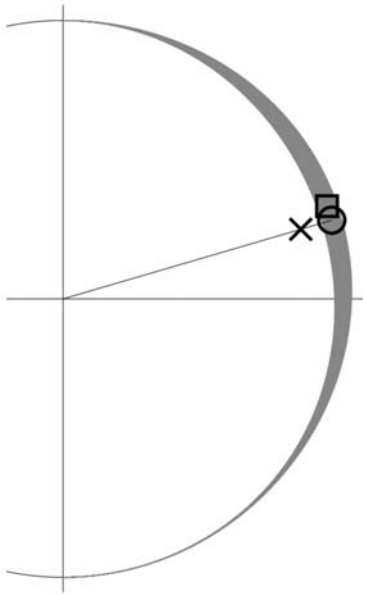

FIG. 3. Constrained Estimation.

The expectation $\bar{\mathbf{x}} = [8/3\pi \;\; 1/4]$, indicated by the cross, clearly violates the norm constraint. The MMSE estimate, indicated by the circle, and the MLE, indicated by the square at $[\sqrt{8}/3 \quad 1/3]$ obey the constraint. We want the "best estimate" of $\mathbf{x}$ to lie on the circle because every point in the probability distribution has this property.

Parallel results hold for the attitude estimation problem. The expectation of the attitude matrix

$$\bar{A} \equiv E[A] \tag{26}$$

will not be an orthogonal matrix in general, i.e. it does not belong to the rotation group SO(3). The MMSE estimate of the attitude matrix is given by

$$\hat{A} \equiv \underset{A' \in \mathrm{SO}(3)}{\arg\min} E[\|A' - A\|_F^2] \tag{27}$$

As in the vector case, we can manipulate this equation to get

$$\begin{aligned} \hat{A} &= \underset{A' \in \mathrm{SO}(3)}{\operatorname{argmin}} \{E[\|A'\|_F^2] - 2E[\operatorname{trace}(A'A^{\mathrm{T}})] + E[\|A\|_F^2]\} \\ &= \underset{A' \in \mathrm{SO}(3)}{\arg\max} \operatorname{trace}(A'\bar{A}^{\mathrm{T}}) \end{aligned} \tag{28}$$

The final equality holds because both A and A' are orthogonal, so their Frobenius norm is equal to the constant 3, and also because trace $(A'\,A^{\mathrm{T}})$ is a linear function of A^{T}. The similarity of this equation and equation (15) means that we can use any of the methods for solving Wahba's Problem to find $\hat{A}$ from $\bar{A}$. Oshman and Carmi have used these concepts in their particle filter developments [29], and I designed an Orthogonal Attitude Filter based on them [31]. The latter has proved to be a very clumsy OAF, however.

For the probability distributions encountered in practical applications, the expectation, MMSE estimate and MLE are all very close, differing by only second order in the spread of the distribution. In general, we want our estimates to satisfy the constraints, so we want the MMSE estimate or MLE rather than the expectation. It isn't clear which if any of these estimates the Extended Kalman Filter (EKF) produces for a nonlinear problem, and we will be rather careless about distinguishing among them.

Quaternions and Kalman Filters

Shortly after the publication of Farrenkopf's note [3], I embarked on a futile attempt to extend his steady-state covariance solution to the three-axis case. It soon became apparent that no closed-form steady-state solution would be forthcoming, but I persisted in developing the general equations. After much effort, I arrived at a formulation that was identical to the Kalman Filter developed by Jim Murrell for the Modular Attitude Control System used on Landsats 4 and 5 [4]. Greatly disappointed, I asked Gene Lefferts if he thought my analysis had any value at all. He said that Malcolm Shuster had developed a parallel analysis, and that our combined work would be worth publishing. The resulting paper is one of the most cited papers that Malcolm or I ever wrote [5]. The final version was written on weekends at Gene's house. He provided the vector measurement model, the only real innovation in the paper, and also served as a buffer to prevent Malcolm and me from coming to blows over disagreements on presentation.

Since the publication of reference [5], much ink has been spilled over the question of how to properly estimate a quaternion [28, 32–38]. We note that a Kalman filter deals with the state estimate and its covariance. The properly normalized MMSE or MLE quaternion estimate is assumed to obey the propagation equation

$$\mathrm{d}\hat{q}\,/\mathrm{d}t = \frac{1}{2}\begin{bmatrix}\hat{\boldsymbol{\omega}}\\ 0\end{bmatrix} \otimes \hat{q} \tag{29}$$

for some $\hat{\boldsymbol{\omega}}$. This preserves the quaternion normalization, so it is not problematical. The measurement update violates the normalization condition in general, however, so care must be taken in the update. A conventional EKF, which we sometimes refer to as an additive EKF (AEKF) defines the quaternion error as

$$\Delta q = q - \bar{q} \tag{30}$$

which has the 4×4 covariance matrix

$$P = E[(\Delta q)\,(\Delta q)^{\mathrm{T}}] \tag{31}$$

The constraint of equation (12) means that

$$\|q\|^2 = \|\bar{q} + \Delta q\|^2 = \|\bar{q}\|^2 + 2(\Delta q)^{\mathrm{T}}\bar{q} + \|\Delta q\|^2 = 1 \tag{32}$$

The expectation of Δq is zero, so the expectation of equation (32) is

$$\|\bar{q}\|^2 + \operatorname{trace} P = 1 \tag{33}$$

Thus

$$\|\bar{q}\| = (1 - \operatorname{trace} P)^{1/2} \tag{34}$$

and the MMSE quaternion estimate is

$$\hat{q} = (1 - \operatorname{trace} P)^{-1/2}\,\bar{q} \tag{35}$$

The main problem in quaternion Kalman filters is shown by considering

$$P\bar{q} = E[(\Delta q)\,(\Delta q)^{\mathrm{T}}\bar{q}] = \frac{1}{2}E[(\Delta q)\,(\operatorname{trace} P - \|\Delta q\|^2)] = -\frac{1}{2}E[\|\Delta q\|^2(\Delta q)] \tag{36}$$

If the probability distribution were symmetric about $\bar{q}$, the right side of this equation would be zero, and P would be singular. However, the norm constraint means that the probability distribution is not symmetric, so P is ill-conditioned but not singular. This has been observed in toy models [28] and numerical studies [38], and analysis indicates that the right side of equation (36) is of order P^2 [34]. It is worth noting that if the norm constraint had been linear, P would have been truly singular.

An ill-conditioned covariance matrix can lead to numerical problems in Kalman filtering, which we want to avoid if at all possible. The rotation group SO(3) has only three degrees of freedom, as was discussed above, so it should be possible to express all the useful quaternion covariance information in a well-conditioned 3×3 matrix. The conceptual advantage of this dimensional reduction, as more truly representing the actual degrees of freedom of the system, has been debated at length [28, 32–38], but the computational advantages are indisputable.

It is possible to avoid the quaternion normalization requirement by parameterizing the attitude matrix as

$$A(q/\|q\|) = \|q\|^{-2}\{(q_4^2 - \|\mathbf{q}\|^2)I_{3\times 3} - 2q_4[\mathbf{q}\times] + 2\mathbf{q}\mathbf{q}^{\mathrm{T}}\} \tag{37}$$

which is an orthogonal matrix regardless of whether the quaternion is normalized [28]. We call this the ray representation, because any quaternion along a ray through the origin corresponds to the same attitude matrix. This approach avoids the complications arising from enforcing the norm constraint, but introduces an unobservable degree of freedom, the quaternion norm. The result is that one eigenvalue of P is unaffected by measurements and thus retains its initial value, which can cause loss of numerical precision if the attitude estimates become very accurate [34]. We will not consider this approach further in this paper.

The next two subsections will consider two specific approaches to quaternion Kalman filtering presented in reference [5]. The EKF analyzed in that reference included gyros used in model replacement mode, which have drift biases that need to be estimated along with the quaternion. We will follow that example and consider the seven-component state vector

$$\mathbf{x} = \begin{bmatrix} q \\ \mathbf{b} \end{bmatrix} \tag{38}$$

where $\mathbf{b}$ is the gyro drift bias vector. If we model dynamics with Euler's equations instead of using gyros in model replacement mode, $\mathbf{b}$ is replaced in the state vector by the angular velocity $\boldsymbol{\omega}$ or angular momentum vector $\mathbf{L}$. The generalization to cases with other components in the state vector is also straightforward, so we will only discuss the seven-dimensional case. Then equation (36) means that there is a null vector

$$\mathbf{x}_{null} = \begin{bmatrix} \hat{q} \\ 0_{3\times 1} \end{bmatrix} \tag{39}$$

for which $P\mathbf{x}_{null}$ is of order P^2. This is not really a null vector of the covariance matrix; it is a vector along the direction of the eigenvalue that leads to the ill-conditioning by being much smaller than the others, as was discussed above.

Multiplicative EKF Approach

The multiplicative EKF (MEKF) represents the true attitude as the quaternion product

$$q = \delta q(\mathbf{a}) \otimes \hat{q} \tag{40}$$

where $\hat{q}$ is the normalized quaternion estimate and $\delta q(\mathbf{a})$ is a unit quaternion representing the quaternion error, parameterized by a three-component representation $\mathbf{a}$ of the error. Three-component representations all have singularities or discontinuities, as was mentioned above, but the MEKF never encounters them because it only uses $\mathbf{a}$ for small attitude errors. The MEKF assumes that $\mathbf{a}$ is chosen so that

$$\delta q(\mathbf{a}) = \begin{bmatrix} \mathbf{a}/2 \\ 1 \end{bmatrix} + \text{order}(\|\mathbf{a}\|^2) \tag{41a}$$

$$A(\delta q(a)) = I_{3\times 3} - [\mathbf{a}\times] + \text{order}(\|\mathbf{a}\|^2) \tag{41b}$$

for rotation matrices close to the identity $I_{3\times 3}$. Specific choices of $\mathbf{a}$ are discussed below. The basic idea of the MEKF is to compute an unconstrained estimate of the three-component $\mathbf{a}$ while using the correctly normalized four-component $\hat{q}$ to provide a globally nonsingular attitude representation [35].

The MEKF incorporates a conventional additive EKF for the six-component state

$$\bar{\mathbf{x}} = \begin{bmatrix} \mathbf{a} \\ \mathbf{b} \end{bmatrix} \tag{42}$$

The discrete measurement update assigns a finite post-update value $\hat{\mathbf{a}}(+)$ to $\mathbf{a}$. Immediately after the measurement update, $\hat{q}$ still retains its pre-update value $\hat{q}(-)$, but equation (40) says that the best estimate of the attitude quaternion is $\delta q(\hat{\mathbf{a}}(+)) \otimes \hat{q}(-)$. A reset procedure in the MEKF corrects this apparent inconsistency by moving the update information from $\hat{\mathbf{a}}(+)$ to a post-update estimate $\hat{q}(+)$ and resetting $\hat{\mathbf{a}}$ to zero. The reset does not change the overall attitude estimate, so equations (40) and (41) require that

$$\hat{q}(+) = \delta q(\hat{\mathbf{a}}(+)) \otimes \hat{q}(-) \tag{43}$$

The update of $\mathbf{b}$ is conventional. If q and $\hat{q}$ obey equations (13) and (29), respectively, with $\hat{\boldsymbol{\omega}}$ chosen appropriately, then $\hat{\mathbf{a}}(t)$ continues to be zero between measurements, so there is no need to propagate it. Both Reynolds [40] and Zanetti et al. [36] have pointed out that the reset modifies the covariance matrix contrary to the assertion in reference [35]. Ignoring this small modification, which is addressed in the Appendix, has not led to any problems in applications, however.

Equations (40) and (41b) imply that

$$A(q) = A(\delta q(\mathbf{a}))A(\hat{q}) \approx (I_{3\times 3} - [\mathbf{a}\times])A(\hat{q}) \tag{44}$$

which is very convenient for computing measurement sensitivity matrices. Choosing $\mathbf{a}$ to be the rotation angle vector, two times the vector part of the quaternion, two times the vector of Rodrigues parameters, or four times the vector of modified Rodrigues parameters [15], gives a stronger relation than equation (41b), namely

$$A(\delta q(\mathbf{a})) = I - [\mathbf{a}\times] + \frac{1}{2}[\mathbf{a}\times]^2 + \text{order}(\|\mathbf{a}\|^3) \tag{45}$$

A vector of asymmetric (e.g. 1–2–3) Euler angles satisfies equation (41b) but not equation (45), and a vector of symmetric (e.g. 3–1–3) Euler angles would satisfy neither [35]. We prefer the Rodrigues parameters (also known as the Gibbs vector), for which

$$\delta q(\mathbf{a}) = (1 + \|\mathbf{a}\|^2/4)^{-1/2} \begin{bmatrix} \mathbf{a}/2 \\ 1 \end{bmatrix} \tag{46}$$

This has both computational and conceptual advantages. The computational advantage is that the reset can avoid the accumulation of roundoff errors by first defining the unnormalized quaternion

$$\hat{q}_{unnorm} \equiv \begin{bmatrix} \hat{\mathbf{a}}(+)/2 \\ 1 \end{bmatrix} \otimes \hat{q}(-) \tag{47}$$

and then updating the unit quaternion by

$$\hat{q}(+) = \hat{q}_{unnorm}/\|\hat{q}_{unnorm}\| \tag{48}$$

The conceptual advantage of the Rodrigues parameters is that they map the rotation group into three-dimensional Euclidean space, with the largest possible 180° attitude errors mapped to points at infinity. Thus probability distributions with infinitely long tails, such as Gaussian distributions, make sense in Rodrigues parameter space. Shuster prefers to take **a** to be two times the rotation angle vector or two times the vector part of δq, and the latter (except for the factor of 2) is the method found in Section XI of reference [5].

The multiplicative error model of the MEKF has been employed in a second-order Kalman filter [35] and an unscented attitude estimator [39].

Covariance Projection Approach

In contrast with the MEKF, the covariance projection approach, which is presented in Section IX of reference [5], is an EKF that estimates the seven-component state vector of equation (38). It is based on the implicit assumption that the estimation errors are orthogonal to the null vector defined by equation (39), i.e.

$$(\Delta\mathbf{x})^{\mathrm{T}}\mathbf{x}_{null} = (\Delta q)^{\mathrm{T}}\hat{q} = 0 \tag{49}$$

This means that instead of assuming the quaternion probability distribution to lie on the unit sphere S3 in four-dimensional quaternion space, we assume that it lies on the three-dimensional hyperplane tangent to S3 at $\hat{q}$. Equations (32) and (49) show that $\bar{q}$ satisfies the quaternion normalization condition to first order, which is an acceptable approximation because the EKF is based on a first-order linearization. It follows from equation (49) that $P\mathbf{x}_{null} = 0_{7\times1}$ exactly, which means that we treat the 7×7 covariance matrix P as if it were singular, in the context of an EKF, even though it is really only ill-conditioned.

The covariance projection approach has no six-dimensional state vector, but it has a six-dimensional state *error* vector, defined as

$$\Delta\tilde{\mathbf{x}} = S^{+}\Delta\mathbf{x} \tag{50}$$

where the 6×7 matrix S^{+} and its 7×6 Moore-Penrose pseudoinverse S satisfy the relations [19, 20]

$$S^{+}S = I_{6\times6} \tag{51a}$$

$$SS^{+} = I_{7\times7} - \mathbf{x}_{null}\mathbf{x}_{null}^{\mathrm{T}} \tag{51b}$$

$$S^{+}\mathbf{x}_{null} = 0_{6\times1} \tag{51c}$$

The seven-component error vector, which is orthogonal to $\mathbf{x}_{null}$ by equation (49), can be recovered by

$$\Delta\mathbf{x} = S\Delta\tilde{\mathbf{x}} \tag{52}$$

which shows that $\Delta\tilde{\mathbf{x}}$ contains all the state error information and that all the covariance information is contained in the well-conditioned 6×6 covariance matrix of the six-dimensional error state

$$\tilde{P} \equiv E[(\Delta\tilde{\mathbf{x}})(\Delta\tilde{\mathbf{x}})^{\mathrm{T}}] = S^{+}P(S^{+})^{\mathrm{T}} \tag{53}$$

Because of equations (49) and (51b), the 7×7 error covariance can be recovered by

$$P = S\tilde{P}S^{\mathrm{T}} \tag{54}$$

For the quaternion estimation problem, S^{+} and S can be given explicitly in terms of the 4×3 matrix

$$\Xi(q) = \begin{bmatrix} q_4 I_{3\times 3} + [\mathbf{q}\times] \\ -\mathbf{q}^T \end{bmatrix} \tag{55}$$

as

$$S = \begin{bmatrix} (1/2)\Xi(\hat{q}) & 0_{4\times 3} \\ 0_{3\times 3} & I_{3\times 3} \end{bmatrix} \tag{56a}$$

$$S^{+} = \begin{bmatrix} 2\Xi^{\mathrm{T}}(\hat{q}) & 0_{3\times 3} \\ 0_{3\times 4} & I_{3\times 3} \end{bmatrix} \tag{56b}$$

These forms differ from those in reference [5] by the factors of $1/2$ and 2 in the upper left corners of S and S^{+}, respectively. This change is made so that the attitude errors are expressed by full angles, to agree with the formulation of the MEKF, rather than by half angles as in reference [5].

The Kalman gain is given in terms of pre-update quantities by equation (1b) and the covariance is updated by equation (1c). To avoid using an ill-conditioned covariance matrix, we substitute equation (54) with the pre-update S matrix into equation (1b), giving

$$K = S(-)\tilde{K} \tag{57}$$

where the subscript i has been omitted to simplify the notation and where $\tilde{K}$ is given by

$$\tilde{K} = \tilde{P}(-)\tilde{H}^{\mathrm{T}}[\tilde{H}\tilde{P}(-)\tilde{H}^{\mathrm{T}} + R]^{-1} \tag{58}$$

with

$$\tilde{H} \equiv HS(-) \tag{59}$$

The seven-component state is propagated by its nonlinear dynamics as in any EKF, and is updated by

$$\hat{\mathbf{x}}(+) = \hat{\mathbf{x}}(-) + K\Delta y = \hat{\mathbf{x}}(-) + S(-)\tilde{K}\Delta y \tag{60}$$

where $\Delta\mathbf{y}$ is the measurement residual.

The covariance update is found by substituting equations (54) and (57) into equation (1c) and using equation (59) to give

$$S(+)\tilde{P}(+)S^{\mathrm{T}}(+) = S(-)\,(I_{6\times 6} - \tilde{K}\tilde{H})\tilde{P}(-)S^{\mathrm{T}}(-) \tag{61}$$

The appearance of $S(+)$ on the left side of this equation and $S(-)$ on the right side reflects the assumption of equation (49) that the pre-update quaternion probability distribution lies on the three-dimensional hyperplane tangent to S3 at $\hat{q}(-)$ while the post-update probability distribution lies on the hyperplane tangent at $\hat{q}(+)$. The two sides of equation (61) have different null vectors, so this equation cannot be exact. The Appendix shows how to treat this disease with a reset of the covariance matrix. The difference between the two null vectors, and therefore between $S(+)$ and $S(-)$, is on the order of the state update, though, so it is customary in the spirit of the linearized EKF to neglect this small difference and write [5]

$$\tilde{P}(+) = (I_{6\times 6} - \tilde{K}\tilde{H})\tilde{P}(-) \tag{62}$$

With this approximation, the matrices $S^{+}(\pm)$ and $S(+)$ are absent from the final EKF formulation, and $S(-)$ appears only in the state update equation. The covariance

propagation and update equations, the measurement sensitivity, and the Kalman gain can all be computed in the six-dimensional representation.

The quaternion update violates quaternion normalization, so equation (48) is used to normalize the updated quaternion. This changes the estimate, but only to second order in the state update, which is acceptable because the EKF is unaware of second-order effects. The overall algorithm is mathematically identical to the MEKF using the state update equations (47) and (48), even though it is based on a very different foundation. The covariance projection idea is conceptually less satisfying than the MEKF, but it is more easily generalized to other constrained estimation problems.

The Importance of Angular Momentum

This is really a subtopic of the previous topic, because conservation of angular momentum is a constraint; but angular momentum deserves a section to itself owing to its importance in spacecraft attitude analysis.

Angular Momentum Parameterization of Attitude

My first aerospace research was with Mel Velez at Goddard. He was pursuing simultaneous orbit/attitude estimation of the spin-stabilized Synchronous Meteorological Satellite (SMS), in order to use the orbit information contained in Earth horizon sensor data. The vastly different time scales of orbit and attitude dynamics impeded progress; orbital equations of motion could be integrated with time steps of tens of minutes, while time steps of fractions of a spin period were required by the rigid-body attitude dynamics. This led Velez to pursue variation-of-parameter approaches to rigid-body dynamics. Harold Morton, John Junkins, and their students had done interesting work in this area [41, 42], but I tried a different approach.

The usual approach is to integrate the equations of motion for the angular momentum in the body frame,

$$\mathrm{d}\mathbf{L}_B/\mathrm{d}t = \mathbf{N}_B - \boldsymbol{\omega} \times \mathbf{L}_B \tag{63}$$

along with equation (13) for the quaternion, where $\mathbf{N}$ denotes the external torque,

$$\boldsymbol{\omega} = J^{-1}(\mathbf{L}_B - \mathbf{L}_{internal}) \tag{64}$$

is the angular velocity, J is the spacecraft's moment of inertia tensor, and $\mathbf{L}_{internal}$ is the angular momentum of any moving internal parts such as reaction wheels. Instead of equation (63), one could integrate the equation of motion for the inertial components of the spacecraft's angular momentum

$$\mathrm{d}\mathbf{L}_I/\mathrm{d}t = \mathbf{N}_I \tag{65}$$

and compute the body frame components as $\mathbf{L}_B = A_{BI}\mathbf{L}_I$. The problem with either of these procedures is that the components of the quaternion are fast variables. My idea was to use both of equations (63) and (65) and not equation (13). The attitude matrix can be parameterized as

$$A_{BI} = R_{BI}R(\mathbf{L}_I/L, \zeta) = R(\mathbf{L}_B/L, \zeta)R_{BI} \tag{66}$$

where R_{BI} is the matrix representing the minimum-angle rotation that takes $\mathbf{L}_I$ into $\mathbf{L}_B$, which is a known function of $\mathbf{L}_I$ and $\mathbf{L}_B$, and $R(\mathbf{e}, \zeta)$ denotes a rotation about the unit vector $\mathbf{e}$ by the angle ζ. The angle variable ζ obeys the fast equation

$$\mathrm{d}\zeta/\mathrm{d}t = L(L^2 + \mathbf{L}_B \cdot \mathbf{L}_I)^{-1}[(\mathbf{L}_B + \mathbf{L}_I) \cdot \boldsymbol{\omega} + L^{-2}(\mathbf{L}_B \times \mathbf{L}_I) \cdot (\mathbf{N}_B + \mathbf{N}_I)] \tag{67}$$

This is quite a bit more complicated than equation (13), but it has the advantage of being a scalar equation. Variation of parameters approaches to attitude dynamics never bore fruit, and these equations (in a cruder form) were put away in a drawer until they found a home in the special issue on Attitude Representations of *The Journal of the Astronautical Sciences* edited by John Junkins and Malcolm Shuster [43].

SpinKF

The angular momentum parameterization had never found widespread use before Joe Sedlak developed an EKF for spinning spacecraft using these variables in 2004 [44]. The state vector

$$\mathbf{x} = \begin{bmatrix} \mathbf{L}_B \\ \mathbf{L}_I \\ \zeta \end{bmatrix} \tag{68}$$

is subject to the nonlinear constraint that the magnitude of the angular momentum is the same in the inertial and body reference frames, that is

$$\|\mathbf{L}_B\| = \|\mathbf{L}_I\| = L \tag{69}$$

This constraint can be expressed to first order as $(\Delta\mathbf{L}_B)^{\mathrm{T}}\hat{\mathbf{L}}_B = (\Delta\mathbf{L}_I)^{\mathrm{T}}\hat{\mathbf{L}}_I$, where the carets denote estimates, not unit vectors. It is handled by the covariance projection technique with the null vector

$$\mathbf{x}_{null} = \frac{1}{\sqrt{2}\,\hat{L}} \begin{bmatrix} \hat{\mathbf{L}}_B \\ -\hat{\mathbf{L}}_I \\ 0 \end{bmatrix} \tag{70}$$

Joe and I have developed several filters in this class, known generically as SpinKF, using different six-component error states [45]. The error state of the best SpinKF variant comprises the vector of infinitesimal attitude error angles and the angular momentum vector in the inertial frame.

Solar, Anomalous, and Magnetospheric Particle Explorer (SAMPEX)

SAMPEX, launched on July 3, 1992, was the first of the Small Explorer (SMEX) series and the first spacecraft I worked on after joining Henry Hoffman's branch of "Satellite Saviors" [46] at Goddard. Its attitude control system, largely defined by Tom Flatley before I entered the picture, uses a single reaction wheel to provide both an angular momentum bias along the spacecraft's Sun-pointing y axis and a torque to control pointing of the science instrument boresights on the z axis (the up direction in Fig. 4) [47, 48]. The momentum bias keeps SAMPEX pointed at the Sun even when the Sun is eclipsed by the Earth. The TRIAD algorithm, or algebraic method [21, 22], computes the attitude matrix using data from a three-axis magnetometer, a two-axis digital Sun sensor, and onboard spacecraft and Sun ephemeris and magnetic field models. SAMPEX uses magnetic torques to damp nutation and keep the y axis pointed at the Sun when the spacecraft is in sunlight. This is accomplished by requiring the total system angular momentum to have a prescribed magnitude L_0 and to be pointed simultaneously along the spacecraft y axis $\mathbf{e}_y$ and along the Sun vector in the body frame $\mathbf{s}_B$. The total system angular momentum in the body frame is given by

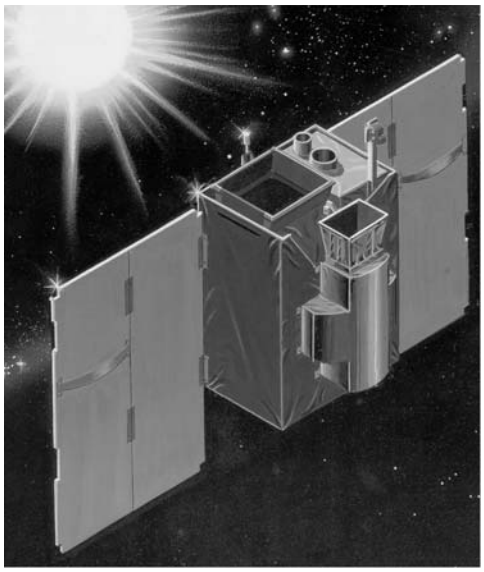

FIG. 4. SAMPEX.

$$\mathbf{L}_B = J\boldsymbol{\omega} + \mathbf{L}_{wheel} \tag{71}$$

with $\mathbf{L}_{wheel}$ computed from reaction wheel tachometer data and the spacecraft angular velocity computed by differentiating the attitude matrix and using equation (6). The unwanted angular momentum

$$\Delta\mathbf{L} = (\mathbf{L}_B - L_0\mathbf{e}_y) + (\mathbf{L}_B - L_0\mathbf{s}_B) \tag{72}$$

is driven toward zero by a magnetic dipole

$$\mathbf{m} = k_{\text{mag}}\Delta\mathbf{L} \times \mathbf{B} \tag{73}$$

where $\mathbf{B}$ is the magnetic field in the body frame.

SAMPEX has far outlived its original lifetime requirement of two years and goal of three years, and its z axis pointing law has been reprogrammed several times over the years to meet changing observational goals [49]. The reaction wheel developed an anomaly on August 17, 2007, after 15 years of flawless operation, and was turned off. SAMPEX is now spin-stabilized, using the magnetic control laws of equations (71)–(73) without any modification, and is still producing useful science data [50].

Hubble Space Telescope (HST)

HST exhibited two problems almost immediately after its release by STS-31 in April 1990. The first was the aberration of its primary mirror, and the second was the appearance of attitude disturbances that were most severe at entry and exit from the Earth's shadow, but that persisted throughout the daylight portion of the orbit. Henry Hoffman immediately attributed these disturbances to thermally induced twisting of the flexible solar arrays, as shown in Fig. 5. Engineers at Goddard, Marshall Space Flight Center, and Lockheed, the HST prime contractor, developed a Solar Array Gain Augmentation algorithm that successfully attenuated these disturbances until the solar arrays were replaced with rigid arrays in 2002.

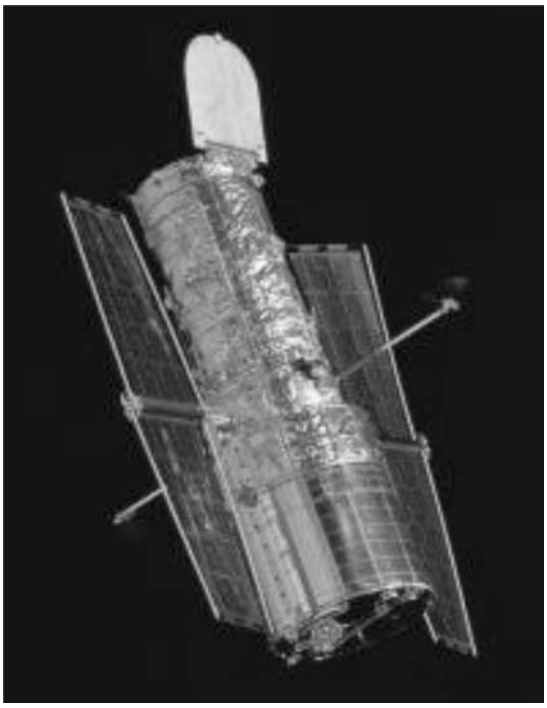

FIG. 5. Hubble Space Telescope.

The next problem to surface on HST was the failure of two of its six precise air-bearing gyros. Failure of two more gyros would have actuated an undesirable firmware controller using limited-life ball-bearing gyros, so the HST Project decided in 1991 to develop a software safe pointing mode requiring fewer than three gyros. We responded to the challenge by developing the Zero-Gyro Sunpoint (ZGSP) mode from initial concept to flight readiness in four months [51]. This mode points a preferred axis toward the Sun during the daylight part of the orbit and establishes a momentum bias in the reaction wheels along the Sun-pointing axis to hold attitude during eclipse, in a manner similar to SAMPEX's science mode. The ZGSP mode does not assume knowledge of an onboard ephemeris or magnetic field model, though, but tries to limit rotation around the Sun line by locking the body to the sensed magnetic field. Orbital motion through the magnetic field causes the body to rotate at a rate that depends on the orientation of the orbit plane, Sun line, and magnetic equator. This can produce a body angular momentum that cancels a significant fraction of the bias momentum. The ZGSP mode has exhibited some large attitude excursions arising from this effect during eclipse, but it maintained HST in a power and thermally safe state for 38 consecutive days between the failure of a fourth gyro in November 1999 and a servicing mission to replace all six gyros.

It warmed my physics-trained heart that Henry Hoffman always emphasized the conservation of angular momentum and was quick to discredit any analysis ignoring this principle, something that I once experienced personally to my great embarrassment. I was delighted to find an application of angular momentum conservation to onboard detection of a spacecraft failure [52]. HST's onboard

computer calculates the total system angular momentum by means of equation (71), with the angular velocity sensed by the gyros. The high torque of the reaction wheels can cause both the wheel angular momentum and the body angular momentum to change rapidly, but their vector sum only changes slowly. After subtracting easily computable gyroscopic and external torques, an apparent disturbance torque is computed as

$$\mathbf{T}_{disturbance} = \mathrm{d}\mathbf{L}_B/\mathrm{d}t + \boldsymbol{\omega} \times \mathbf{L}_B - \mathbf{m} \times \mathbf{B} - \mathbf{T}_{gravity\text{-}gradient} \tag{74}$$

A large value of this disturbance torque indicates a failure of either a reaction wheel tachometer or a gyro. A tachometer failure can be identified by an independent test, so we implemented this system momentum test to identify gyro failures. It initiated entry to ZGSP mode three times in late 2002 and early 2003.

Wilkinson Microwave Anisotropy Probe (WMAP)

A GSFC-Princeton University collaboration formed in 1994 proposed MAP as a Mid-Sized Explorer (MIDEX) mission to measure the anisotropy of the cosmic microwave background radiation with more resolution and precision than the Differential Microwave Radiometer (DMR) instrument on Goddard's Cosmic Background Explorer (COBE) spacecraft. The Principal Investigator (PI) of MAP was Chuck Bennett of GSFC, who had been deputy PI on DMR. The Princeton team included David Wilkinson, the dean of cosmic microwave background studies, in whose honor MAP was rechristened WMAP in 2002.

The need for a highly interconnected set of measurements over an annulus between 45° and 90° from the anti-Sun line requires WMAP to execute a fast spin at about 0.5 rpm and a slow precession of its spin axis at one revolution per hour at a constant angle of 22.5° from the anti-Sun line. This scan pattern, similar to that of COBE, could be easily represented by 3-1-3 Euler angles, as Ed Seidewitz and I had noticed during the development of ADEAS. John Crassidis, who was working with me as a National Research Council Resident Research Associate, used MATLAB to display this pattern in the "spirograph" shown in Fig. 6. Tom Flatley tried without success to find a dual-spin dynamical configuration that could provide this scan pattern passively—and I believed that if he couldn't, nobody could—so we designed WMAP as an actively controlled zero-momentum spacecraft. MIDEXs were to be single-string spacecraft, so three reaction wheels on WMAP serve the dual functions of counterbalancing the body's spin angular momentum to maintain zero system momentum and applying control torques to provide the desired attitude. The wheel axis orientations are chosen to bias all wheel speeds away from zero to avoid undesirable zero-speed crossings. WMAP, shown in Fig. 7, was launched in 2001 as the second MIDEX mission [53].

The scan motion of WMAP causes the Sun vector in its body frame to describe a circle with radius varying between 22.44° and 22.54°. I have characterized a picture of this circle generated from flight Digital Sun Sensor data as the least interesting figure in any paper [53]. The picture got a lot more interesting on February 17, 2005, when the daily telemetry contact revealed WMAP to be in Safehold mode with one reaction wheel turned off and with flags indicating that several failures had been detected, including failure of the system momentum test. A replay of the Coarse Sun Sensor data showed that the Sun had followed the path plotted in Fig. 8, going as much as 45° off the spin axis and ending up on the spin axis 15 minutes

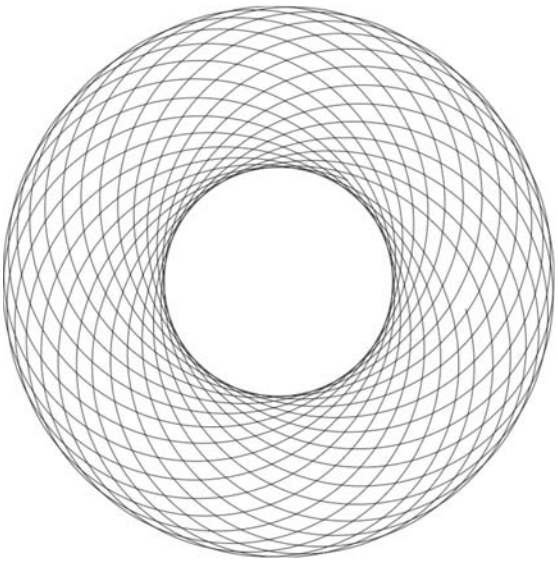

FIG. 6. WMAP Scan Pattern.

later. Note that the jagged path is an artifact of the sparsity of the data and does not reflect the true motion and that the Coarse Sun Sensor outputs are not simply the transverse components of the unit vector. Figure 8 shows that the Safehold mode behaved as designed, using two wheels to drive the Sun to the spin axis while giving up control of the spin rate.

There were two concerns. The first was that the reaction wheel had suffered a mechanical failure that would prevent WMAP from successfully continuing its mission. This concern was laid to rest by an examination of Fig. 9 showing the time history

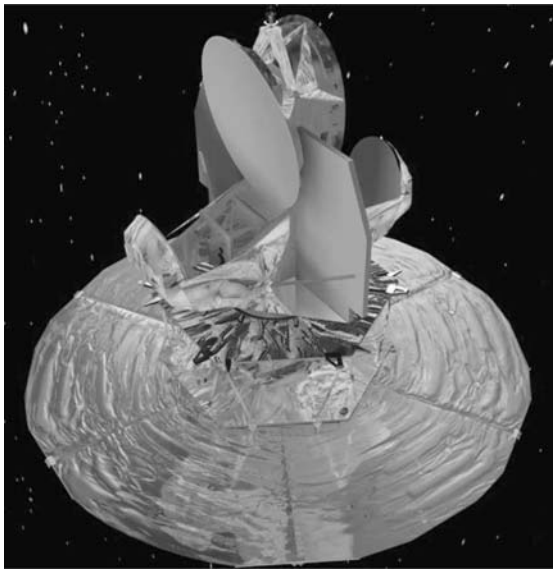

FIG. 7. WMAP.

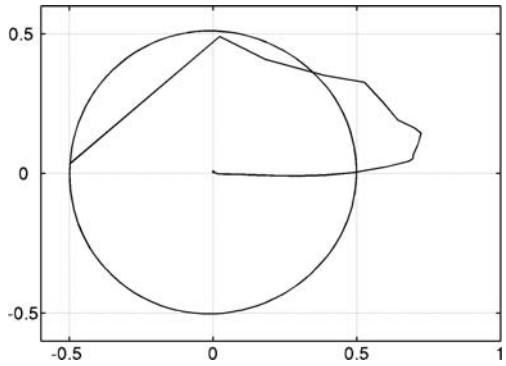

FIG. 8. Sun Unit Vector in WMAP Body Frame (Coarse Sun Sensor Units).

of WMAP's total system angular momentum, which is computed onboard using equation (71) with the angular velocity sensed by the gyros. The sudden jump at about 10 minutes cannot possibly be a real change in the system angular momentum, so it must reflect either a loss of wheel tachometer data or of gyro data. The observation that the system momentum after 40 minutes is equal to the system momentum before the jump also leads to the conclusion that this is the true, nearly constant, system momentum. Suspicion centered on the tachometer because 15 Nms is the amount stored in one wheel to counteract the spin momentum, and 30 minutes is a typical time for a wheel to run down if power is removed. Further examination of the telemetry exonerated the tachometer, too. It turns out that a cosmic ray upset had caused the power supply electronics to accidentally turn off the reaction wheel.

The second concern was that the large excursion of the Sun from the spin axis could have caused damage to the reflectors, which were passively cooled to about 90°K and protected by the sunshield shown in Fig. 7 for excursions of no more than 25°. However, successful recovery from Safehold mode showed that the reflectors had suffered no damage, and WMAP continues to provide data that have enabled scientists to answer key questions about the origin of structure in the early universe and the fate of the universe.

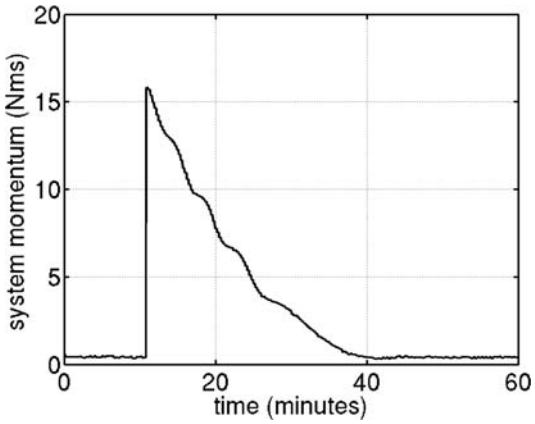

FIG. 9. WMAP System Angular Momentum.

Conclusions

My aerospace career has been extremely satisfying, but my greatest reward has been the opportunity to work with incredibly talented colleagues. I look back on my career as having been largely fortuitous—a matter of being in the right place at the right time—but also of seizing the opportunities offered to me. I still see WMAP as its high point. It gave me the opportunity to begin an attitude control system design with a clean sheet of paper, and also to play a small role in determining the age of the universe.

My career did not end with WMAP, of course. I could mention Swift, a MIDEX spacecraft launched in 2004 that uses six reaction wheels to slew 60° in 60 seconds to catch elusive short-lived gamma-ray bursts on the fly. I continue to follow HST, which has used a two-gyro fine-pointing mode to save its other remaining operable gyro while continuing to carry out its mission. A one-gyro fine-pointing mode with equivalent performance is available in case it is needed in the future. I have been heavily involved in the development of the James Webb Space Telescope, particularly in dealing with the complications arising from the solar radiation pressure torque on its tennis-court-sized sunshield. I have largely been an interested observer and friendly critic of these developments, however. The torch has been passed to a new generation.

Acknowledgments

I will not attempt to list the names of the many colleagues who have encouraged me, instructed me, inspired me, and spurred me on. Many, but not all, can be found in this paper or as authors of the cited references. I trust that you all know who you are. I owe a great debt of gratitude to all of you.

References

[1] MARKLEY, F. L. "Humble Problems," presented as paper AAS 06-238 at the 2006 AAS/AIAA Space Flight Mechanics Meeting, San Diego, CA, 2006; *Advances in the Astronautical Sciences,* Vol. 124, Part II, 2006, pp. 2205–2222.

[2] CRASSIDIS, J. L. and JUNKINS, J. L. *Optimal Estimation of Dynamic Systems*, Chapman & Hall/CRC, Boca Raton, FL, 2004, Chapter 5.

[3] FARRENKOPF, R. L. "Analytic Steady-State Accuracy Solutions for Two Common Spacecraft Attitude Estimators," *Journal of Guidance and Control*, Vol. 1, No. 4, 1978, pp. 282–284.

[4] MURRELL, J. W. "Precision Attitude Determination for Multimission Spacecraft," presented as paper AIAA 78-1248 at the 1978 AIAA Guidance and Control Conference, Palo Alto, CA, August 1978, pp. 70–87.

[5] LEFFERTS, E. J., MARKLEY, F. L., and SHUSTER, M. D. "Kalman Filtering for Spacecraft Attitude Estimation," *Journal of Guidance, Control, and Dynamics*, Vol. 5, No. 5, 1982, pp. 417–429.

[6] FALLON, III, L. "Gyroscope Models," in *Spacecraft Attitude Determination and Control*, J. R. Wertz, ed., D. Reidel, Dordrecht, Holland, 1978, pp. 266–270.

[7] MARKLEY, F. L. and REYNOLDS, R. R. "Analytic Steady-State Accuracy of a Spacecraft Attitude Estimator," *Journal of Guidance, Control, and Dynamics*, Vol. 23, No. 6, 2000, pp. 1065–1067.

[8] MARKLEY, F. L., SEIDEWITZ, E., and DEUTSCHMANN, J. "Attitude Determination Error Analysis: General Model and Specific Application," *Mécanique Spatiale: Space Dynamic*s, Cepadues-Editions, Toulouse, France, 1989, pp. 251–266.

[9] MARKLEY, F. L. and CARPENTER, J. R. "Generalized Linear Covariance Analysis," *The Journal of the Astronautical Sciences,* Vol. 57, Nos. 1 & 2, 2009. (this issue)

[10] BAUER, F. H., FEMIANO, M. D., and MOSIER, G. E. "Attitude Control System Conceptual Design for the X-Ray Timing Explorer," presented as paper AIAA 92-4334 at the 1992 AIAA Guidance, Navigation, and Control Conference, Hilton Head Island, SC, August 1992, pp. 236–250.

[11] SEDLAK, J. and HASHMALL, J. "Accurate Magnetometer/Gyroscope Attitudes Using a Filter with Correlated Sensor Noise," *Proceedings of the 1997 Flight Mechanics Symposium,* NASA Conference Publication 3345, Greenbelt, MD, 1976, pp. 83–87.

[12] ANDREWS, S. F. and BILANOW, S. "Recent Flight Results of the TRMM Kalman Filter," presented as paper AIAA 2002-5047 at the 2002 AIAA Guidance, Navigation, and Control Conference, Monterey, CA, August 2002.

[13] MARKLEY, F. L. and BAR-ITZHACK, I. Y. "Unconstrained Optimal Transformation Matrix," *IEEE Transactions on Aerospace and Electronic System*, Vol. 34, No. 1, 1998, pp. 338–340.

[14] MARKLEY, F. L. "Equations of Motion," in *Spacecraft Attitude Determination and Control*, J. R. Wertz, ed., D. Reidel, Dordrecht, Holland, 1978, pp. 510–523.

[15] SHUSTER, M. D. "A Survey of Attitude Representations," *The Journal of the Astronautical Sciences*, Vol. 41, No. 4, 1993, pp. 439–517.

[16] MARKLEY, F. L. "Parameterization of the Attitude," in *Spacecraft Attitude Determination and Control*, J. R. Wertz, ed., D. Reidel, Dordrecht, Holland, 1978, pp. 410–420.

[17] STUELPNAGEL, J. "On the Parameterization of the Three-Dimensional Rotation Group," *SIAM Review*, Vol. 6, No. 4, 1964, pp. 422–430.

[18] WAHBA, G. "A Least Squares Estimate of Spacecraft Attitude," *SIAM Review*, Vol. 7, No. 3, 1965, p. 409.

[19] HORN, R. A. and JOHNSON, C. R. *Matrix Analysis*, Cambridge, UK, Cambridge University Press, 1985.

[20] GOLUB, G. H. and VAN LOAN, C. F. *Matrix Computations*, Baltimore, MD, The Johns Hopkins University Press, 1983.

[21] LERNER, G. M. "Three-Axis Attitude Determination," in *Spacecraft Attitude Determination and Control*, J. R. Wertz, ed., D. Reidel, Dordrecht, Holland, 1978, pp. 420–428.

[22] SHUSTER, M. D. and OH, S. D. "Three-Axis Attitude Determination from Vector Observations," *Journal of Guidance and Control*, Vol. 4, No. 1, 1981, pp. 70–77.

[23] MARKLEY, F. L. "Attitude Determination Using Vector Observations and the Singular Value Decomposition," *The Journal of the Astronautical Sciences*, Vol. 36, No. 3, 1988, pp. 245–258.

[24] MARKLEY, F. L. "Attitude Determination Using Vector Observations: a Fast Optimal Matrix Algorithm," *The Journal of the Astronautical Sciences*, Vol. 41, No. 2, 1993, pp. 261–280.

[25] MORTARI, D. "ESOQ: A Closed-Form Solution to the Wahba Problem," *The Journal of the Astronautical Sciences*, Vol. 45, No. 2, 1997, pp. 195–204.

[26] MORTARI, D. "Second Estimator of the Optimal Quaternion," *Journal of Guidance, Control, and Dynamics*, Vol. 23, No. 5, 2000, pp. 885–888.

[27] MARKLEY, F. L. and MORTARI, D. "Quaternion Attitude Estimation Using Vector Observations," *The Journal of the Astronautical Sciences*, Vol. 48, No. 2/3, 2000, pp. 359–380.

[28] MARKLEY, F. L. "Attitude Estimation or Quaternion Estimation?" *The Journal of the Astronautical Sciences,* Vol. 52, No. 1/2, 2004, pp. 221–238.

[29] OSHMAN, Y. and CARMI, A. "Attitude Estimation from Vector Observations Using a Genetic-Algorithm-Embedded Quaternion Particle Filter," *Journal of Guidance, Control, and Dynamics*, Vol. 29, No. 4, 2006, pp. 879–891.

[30] SHUSTER, M. D. "Maximum Likelihood Estimate of Spacecraft Attitude," *The Journal of the Astronautical Sciences*, Vol. 37, No. 1, 1989, pp. 79–88.

[31] MARKLEY, F. L. "Attitude Filtering on SO(3)," *The Journal of the Astronautical Sciences*, Vol. 54, No. 3/4, 2006, pp. 391–413.

[32] SHUSTER, M. D. "Constraint in Attitude Estimation Part I: Constrained Estimation," *The Journal of the Astronautical Sciences,* Vol. 51, No. 1, 2003, pp. 51–74.

[33] SHUSTER, M. D. "Constraint in Attitude Estimation Part II: Unconstrained Estimation," *The Journal of the Astronautical Sciences,* Vol. 51, No. 1, 2003, pp. 75–101.

[34] PITTELKAU, M. E. "An Analysis of the Quaternion Attitude Determination Filter," *The Journal of the Astronautical Sciences*, Vol. 51, No. 1, 2003, pp. 103–120.

[35] MARKLEY, F. L. "Attitude Error Representations for Kalman Filtering," *Journal of Guidance, Control, and Dynamics*, Vol. 26, No. 2, 2003, pp. 311–317.

[36] ZANETTI, R., MAJJI, M., BISHOP, R. H., and MORTARI, D. "Norm Constrained Kalman Filtering," *Journal of Guidance, Control, and Dynamics*, Vol. 32, No. 5, 2009, pp. 1458–1465.

[37] CALISE, A. J. "Enforcing an Algebraic Constraint in Extended Kalman Filter Design," presented as paper AIAA 2007-6515 at the 2007 AIAA Guidance, Navigation, and Control Conference, Hilton Head, SC, August 2007.

[38] CARMI, A. and OSHMAN, Y. "Asymptotic Behavior of the Estimation Error Covariance of

Quaternion Estimators," *Journal of Guidance, Control, and Dynamics*, Vol. 31, No. 6, 2008, pp. 1665–1676.
[39] CRASSIDIS, J. L. and MARKLEY, F. L. "Unscented Filtering for Spacecraft Attitude Estimation," *Journal of Guidance, Control, and Dynamics*, Vol. 26, No. 4, 2003, pp. 536–542.
[40] REYNOLDS, R. G. "Asymptotically Optimal Attitude Filtering with Guaranteed Convergence," *Journal of Guidance, Control, and Dynamics*, Vol. 31, No. 1, 2008, pp. 114–122.
[41] MORTON, H. S., Jr., JUNKINS, J. L., and BLANTON, J. N. "Analytical Solutions for Euler Parameters," *Celestial Mechanics*, Vol. 10, 1974, pp. 287–301.
[42] KRAIGE, L. G. and JUNKINS, J. L. "Perturbation Formulations for Satellite Attitude Dynamics," *Celestial Mechanics*, Vol. 13, 1976, pp. 39–64.
[43] MARKLEY, F. L. "New Dynamic Variables for Momentum-Bias Spacecraft," *The Journal of the Astronautical Sciences*, Vol. 41, No. 4, 1993, pp. 557–567.
[44] SEDLAK, J. E. "Spinning Spacecraft Attitude Estimation Using Markley Variables: Filter Implementation and Results," *Proceedings of the 2005 Flight Mechanics Symposium*, Goddard Space Flight Center, Greenbelt, MD, NASA Conference Publication NASA/CP-2005-212789, October 2005.
[45] MARKLEY, F. L. and SEDLAK, J. E. "Kalman Filter for Spinning Spacecraft Attitude Estimation," *Journal of Guidance, Control, and Dynamics*, Vol. 31, No. 6, 2008, pp. 1750–1760.
[46] KUZNIK, F. "Satellite Saviors," *AIR & SPACE/Smithsonian*, Vol. 6, No. 3, 1991, pp. 66–70.
[47] FLATLEY, T. W., FORDEN, J. K., HENRETTY, D. A., LIGHTSEY, E. G., and MARKLEY, F. L. "Onboard Attitude Determination and Control Algorithms for SAMPEX," *Proceedings of the 1990 Flight Mechanics/ Estimation Theory Symposium*, Goddard Space Flight Center, Greenbelt, MD, NASA Conference Publication 3102, May 1990, pp. 379–398.
[48] MCCULLOUGH, J. D., FLATLEY, T. W., HENRETTY, D. A., MARKLEY, F. L., and SAN, J. K. "Testing of the Onboard Attitude Determination and Control Algorithms for SAMPEX," *Proceedings of the 1992 Flight Mechanics/ Estimation Theory Symposium*, Goddard Space Flight Center, Greenbelt, MD, May 1992, NASA Conference Publication 3186, pp. 55–68.
[49] MARKLEY, F. L., FLATLEY, T. W. and LEOUTSAKOS, T. "SAMPEX Special Pointing Mode," *Proceedings of the 1995 Flight Mechanics/Estimation Theory Symposium*, Goddard Space Flight Center, Greenbelt, MD, May 1995, NASA Conference Publication 3299, pp. 201–215.
[50] TSAI, D. C., MARKLEY, F. L., and WATSON, T. P. "SAMPEX Recovery to Spin Stabilized Mode," *SpaceOps 2008*, Heidelberg, Germany, May 12–16, 2008.
[51] MARKLEY, F. L. and NELSON, J. D. "Zero-Gyro Safemode Controller for the Hubble Space Telescope," *Journal of Guidance, Control, and Dynamics,* Vol. 17, No. 4, 1994, pp. 815–822.
[52] MARKLEY, F. L., KENNEDY, K. R., NELSON, J. D., and MOY, E. W. "Autonomous Spacecraft Gyro Failure Detection Based on Conservation of Angular Momentum," *Journal of Guidance, Control, and Dynamics,* Vol. 17, No. 6, 1994, pp. 1385–1387.
[53] MARKLEY, F. L., ANDREWS, S. F., O'DONNELL, J. R., Jr., and WARD, D. K. "Attitude Control System of the Wilkinson Microwave Anisotropy Probe," *Journal of Guidance, Control, and Dynamics*, Vol. 28, No. 3, 2005, pp. 385–397.

Appendix: Reset of the Quaternion Covariance Matrix

Multiplicative EKF

After the reset, the quaternion covariance in the MEKF should be the covariance of the reset attitude error vector referenced to $\hat{q}(+)$, which we will denote $\mathbf{a}(++)$. We denote the pre-reset attitude error vector referenced to $\hat{q}(-)$ by $\mathbf{a}(+)$. The true quaternion doesn't care about the reference, so equations (40) and (43) give

$$\begin{aligned} q &= \delta q(\mathbf{a}(+)) \otimes \hat{q}(-) = \delta q(\mathbf{a}(++)) \otimes \hat{q}(+) \\ &= \delta q(\mathbf{a}(++)) \otimes \delta q(\hat{\mathbf{a}}(+)) \otimes \hat{q}(-) \end{aligned} \tag{A1}$$

This means that $\delta q(\mathbf{a}(+)) = \delta q(\mathbf{a}(++)) \otimes \delta q(\hat{\mathbf{a}}(+))$, or

$$\delta q(\mathbf{a}(++)) = \delta q(\mathbf{a}(+)) \otimes \delta q(-\hat{\mathbf{a}}(+)) \tag{A2}$$

All three-parameter error representations obeying equation (41a) will give the same covariance reset to first order in $\|\hat{\mathbf{a}}(+)\|$, but will differ in higher orders. It is not clear, though, that the higher orders are significant. If we use the preferred Rodrigues parameter representation given by equation (46), equation (A2) is equivalent to the product rule for the Rodrigues parameters [15, 16]

$$\rho'' = (1 - \rho' \cdot \rho)^{-1}(\rho' + \rho - \rho' \times \rho) \tag{A3}$$

with $\rho'' = \mathbf{a}(++)/2$, $\rho' = \mathbf{a}(+)/2$, and $\rho = -\hat{\mathbf{a}}(+)/2$. This gives

$$\begin{aligned}\mathbf{a}(++) &= [1 + (1/4)\,\mathbf{a}(+) \cdot \hat{\mathbf{a}}(+)]^{-1}[\mathbf{a}(+) - \hat{\mathbf{a}}(+) + (1/2)\,\mathbf{a}(+) \times \hat{\mathbf{a}}(+)] \\ &= \{1 - [4 + \mathbf{a}(+) \cdot \hat{\mathbf{a}}(+)]^{-1}[\hat{\mathbf{a}}(+) \cdot \Delta\mathbf{a}(+)]\} M\Delta\mathbf{a}(+)\end{aligned} \tag{A4}$$

where $\Delta\mathbf{a}(+) \equiv \mathbf{a}(+) - \hat{\mathbf{a}}(+)$ and

$$M \equiv (1 + \|\hat{\mathbf{a}}(+)\|^2/4)^{-1}\{I_{3\times 3} - [\hat{\mathbf{a}}(+)\times]/2\} \tag{A5}$$

Ignoring terms of second and higher orders in $\Delta\mathbf{a}(+)$ in equation (A4), which is consistent with the usual assumptions made in an EKF, and remembering that $\hat{\mathbf{a}}(++) \equiv 0$ by the definition of the reset gives

$$\Delta\mathbf{a}(++) \equiv \mathbf{a}(++) - \hat{\mathbf{a}}(++) = M\Delta\mathbf{a}(+) \tag{A6}$$

The vector $\mathbf{b}$ is unaffected by the reset, so the covariance of the six-dimensional state of equation (42) must be reset by

$$\tilde{P}(++) = \begin{bmatrix} M & 0_{3\times 3} \\ 0_{3\times 3} & I_{3\times 3} \end{bmatrix} \tilde{P}(+) \begin{bmatrix} M & 0_{3\times 3} \\ 0_{3\times 3} & I_{3\times 3} \end{bmatrix}^{\mathrm{T}} \tag{A7}$$

Covariance Projection Method

If equation (61) were true, then equation (51a) would give

$$\tilde{P}(+) = [S^{+}(+)S(-)](I_{6\times 6} - \tilde{K}\tilde{H})\tilde{P}(-)[S^{+}(+)S(-)]^{\mathrm{T}} \tag{A8}$$

This equation, unlike equation (61), has no diseases. We use it to define the reset covariance $\tilde{P}(++)$ to be the quantity on the left side, and retain the notation $\tilde{P}(+)$ for the updated covariance defined by equation (62) that appears on the right side. Then with equations (56a) and (56b), we have

$$\tilde{P}(++) = \begin{bmatrix} \Xi^{\mathrm{T}}(+)\Xi(-) & 0_{3\times 3} \\ 0_{3\times 3} & I_{3\times 3} \end{bmatrix} \tilde{P}(+) \begin{bmatrix} \Xi^{\mathrm{T}}(+)\Xi(-) & 0_{3\times 3} \\ 0_{3\times 3} & I_{3\times 3} \end{bmatrix}^{\mathrm{T}} \tag{A9}$$

Equation (55) and some quaternion algebra [15] give

$$\Xi^{\mathrm{T}}(+)\Xi(-) = (\delta\hat{q}_4)I_{3\times 3} - [\boldsymbol{\delta}\hat{\mathbf{q}}\times] \tag{A10}$$

where, with equation (46)

$$\delta\hat{q} = \begin{bmatrix} \boldsymbol{\delta}\hat{\mathbf{q}} \\ \delta\hat{q}_4 \end{bmatrix} = \hat{q}(+) \otimes \hat{q}^{-1}(-) = (1 + \|\hat{\mathbf{a}}(+)\|^2/4)^{-1/2} \begin{bmatrix} \hat{\mathbf{a}}(+)/2 \\ 1 \end{bmatrix} \tag{A11}$$

Combining these equations gives

$$\Xi^{\mathrm{T}}(+)\Xi(-) = (1 + \|\hat{\mathbf{a}}(+)\|^2/4)^{-1/2}\{I_{3\times 3} - [\hat{\mathbf{a}}(+)\times]/2\} \tag{A12}$$

The normalization of the updated quaternion discussed below equation (62) provides another correction factor of $(1 + \|\hat{\mathbf{a}}(+)\|^2/4)^{-1/2}$, and inserting this factor and equation (A12) into equation (A9) recovers equation (A7) exactly. Thus the reset correction to the covariance matrix is the same in the MEKF and covariance projection approach to at least second order in $\|\hat{\mathbf{a}}(+)\|$.